

The Intrinsic Fatigue Mechanism of the Porcine Aortic Valve Extracellular Matrix

Jun Liao, Erinn M. Joyce, W. David Merryman, Hugh L. Jones, Mina Tahai, M. F. Horstemeyer, Lakiesha N. Williams, Richard A. Hopkins, et al.

Cardiovascular Engineering and Technology

ISSN 1869-408X

Cardiovasc Eng Tech
DOI 10.1007/s13239-011-0080-4



Your article is protected by copyright and all rights are held exclusively by Biomedical Engineering Society. This e-offprint is for personal use only and shall not be self-archived in electronic repositories. If you wish to self-archive your work, please use the accepted author's version for posting to your own website or your institution's repository. You may further deposit the accepted author's version on a funder's repository at a funder's request, provided it is not made publicly available until 12 months after publication.

The Intrinsic Fatigue Mechanism of the Porcine Aortic Valve Extracellular Matrix

JUN LIAO,¹ ERINN M. JOYCE,² W. DAVID MERRYMAN,³ HUGH L. JONES,¹ MINA TAHAI,¹
M. F. HORSTEMEYER,¹ LAKIESHA N. WILLIAMS,¹ RICHARD A. HOPKINS,⁴ and MICHAEL S. SACKS²

¹Tissue Bioengineering Laboratory, Department of Agricultural and Biological Engineering, Computational Manufacturing and Design, CAVS, Mississippi State University, 130 Creelman Street, Mississippi State, MS 39762, USA; ²Department of Bioengineering and McGowan Institute for Regenerative Medicine, Cardiovascular Biomechanics Laboratory, University of Pittsburgh, Pittsburgh, PA 15219, USA; ³Department of Biomedical Engineering, Vanderbilt University, Nashville, TN 37235, USA; and ⁴Department of Cardiac Surgery, Children's Mercy Hospital and Clinics, Kansas City, MO 64108, USA

(Received 20 April 2011; accepted 22 December 2011)

Associate Editor Ajit P. Yoganathan oversaw the review of this article.

Abstract—Decellularized aortic valves (AV) are promising scaffolds for tissue engineered heart valve (TEHV) application; however, it is not known what the intrinsic fatigue mechanism of the AV extracellular matrix (ECM) is and how this relates to decellularized AV functional limits when tissue remodeling does not take place. In this study, decellularized AVs were subjected to in vitro cardiac exercising and the exercised leaflets were characterized to assess the structural and mechanical alterations. A flow-loop cardiac exerciser was designed to allow for pulsatile flow conditions while maintaining sterility. The acellular valve conduits were sutured into a silicone root with the Valsalva sinus design and subjected to cardiac cycling for 2 weeks (1.0 million cycles) and 4 weeks (2.0 million cycles). Following exercising, thorough structural and mechanical characterizations were then performed. The overall morphology was maintained and the exercised leaflets were able to coapt and support load; however, the leaflets exhibited an unfolded and thinned morphology. The straightening of the locally wavy collagen fiber structure was confirmed by histology and small angle light scattering; the disruption of elastin network was also observed. Biaxial mechanical testing showed that the leaflet extensibility was largely reduced by cardiac exercising. In the absence of cellular maintenance, decellularized leaflets experience structural fatigue due to lack of exogenous stabilizing crosslinks, and the structural disruption is irreversible and cumulative. Although not being a means to predict the durability of the acellular valve implants, this mechanistic study reveals the fatigue pattern of the acellular leaflets and implies the importance of recellularization in developing a TEHV, in which long term durability will likely be better achieved by continual remodeling and repair of the valvular ECM.

Keywords—Aortic valve leaflet, Extracellular matrix, Decellularization, Cyclic fatigue, Tissue engineering.

INTRODUCTION

The function of the aortic valve (AV) is to maintain unidirectional blood flow from the left ventricle to the aorta. In systolic phase, the three leaflets of the AV are opened to allow blood to flow from the left ventricle to the aorta; in the diastolic phase, the three leaflets are closed to prevent blood in the aorta from leaking back into the ventricle. The aortic valve leaflet (AVL) has a trilayered structure that provides optimal performance and fatigue resistance over the lifespan.³⁷ However, diseases or abnormalities of AV disturb the optimal performance and result in aortic stenosis or aortic insufficiency. Dysfunctional AV need to be replaced surgically with mechanical valves, bioprosthetic valves, and homografts to avoid cardiopulmonary failures. It is reported that over 300,000 valve replacement surgeries are preformed worldwide each year.⁴²

Among the valve replacements, mechanical valves consist of synthetic materials and therefore have better durability (~25 years) than bioprosthetic valves.²⁹ However, because the mechanical valves are thrombogenic, the patient must endure the associated side effects of anticoagulation therapies to combat thrombosis and thromboembolism.^{23,27} Bioprosthetic valves are made of bovine pericardium or porcine AV that are treated with glutaraldehyde to effectively crosslink collagen scaffolds and inhibit tissue degradation. Patients that receive bioprosthetic valves generally have low

Address correspondence to Jun Liao, Tissue Bioengineering Laboratory, Department of Agricultural and Biological Engineering, Computational Manufacturing and Design, CAVS, Mississippi State University, 130 Creelman Street, Mississippi State, MS 39762, USA. Electronic mail: jlliao@abe.msstate.edu

immunologic responses and do not require prolonged anticoagulant therapies. However, glutaraldehyde-fixed tissues experience structural fatigue, which is coupled with the calcification of extracellular matrix (ECM), leading to stenosis or aortic insufficiency.²⁷ Bioprosthetic valves are commonly replaced within 10 years and as soon as 5 years in younger patients.²⁷ Another alternative for valve replacement is allogeneic transplant (homograft). According to Angell *et al.*, the cryopreserved homograft had viable cells at the time of implantation, but viable cells were found to reduce and eventually lose with time.¹ Although showing good hemodynamics at early time, cryopreserved homografts exhibited a disappointing durability in the pediatric population.^{1,22,41} Most of all, for current valve substitutes, the inability to grow in pediatric recipients leads to risky multiple valve replacement operations.^{5,12,25,28}

Tissue engineering is a promising approach to develop a valve substitute containing autologous viable cells and with growth potential for the pediatric population. Ideally, the tissue engineered heart valve (TEHV) will be able to grow along with patient's somatic growth and remodel to maintain the optimal functionality under various hemodynamic conditions. Currently, both synthetic and tissue-derived scaffolds are used for TEHV.³⁶ In the synthetic approach, biodegradable and bioresorbable polymeric scaffolds, such as polyglycolic acid (PGA), polylactic acid (PLA), polyhydroxyoctanoate (PHO), were molded into heart valve geometry and seeded with cells isolated and expanded from donor tissue.^{13,30,31} Up to now, synthetic scaffolds have not been used for high pressure left ventricular outflow replacement.³⁵ It is still an ongoing effort to identify the ideal biodegradable polymeric scaffold material that is suitable for valve construction, has sufficient mechanical properties, and is resorbable within 6 weeks without stimulating inflammatory scar formation.^{13,30,31}

Recently, decellularized natural aortic and pulmonary valve tissues have been used for TEHV.^{2,4,6,7,15,34,39,44} It has been shown that natural ligands and ECM constituents of the decellularized valve tissues benefit the cell attachment, endothelialization and tissue reconstitution.³⁴ Another benefit of decellularization approach is that tissue-derived scaffolds circumvent the valve functional design issues by preserving a template of native valve leaflets. Moreover, in the acellular scaffold, immunogenicity of collagen (the most abundant component) is very low due to the small species difference among different type I collagens.⁴³ No immunological response was shown when acellular valvular and vascular grafts were implanted in dogs.^{39,40} Various detergents or enzymatic agents have been used to remove cells and cellular debris in heart valves. They are non-ionic detergent

Triton X-100 (tert-octylphenylpolyoxyethylen),^{2,3,39} anionic detergent SDS (sodium dodecyl sulfate),¹⁵ cationic detergent CPC (*N*-cetylpyridinium chloride),³² and enzymatic agent Trypsin.^{6,11,33,34,44} The above detergents or enzymatic agents are often used with DNase, RNase A, phospholipases, and ethylenediaminetetraacetic acid (EDTA).

Many factors determine the successful outcome for decellularized tissues used in heart valve replacements. Currently, potential decellularization procedures are evaluated using trial-and-error approaches that involve time consuming and expensive chronic animal studies.^{32,34,38,39} As an example, the best scenario one can envisage is a successful reseeding followed by tissue maintenance in the valve implants; however, one might ask what if the reseeded cells in TEHV reduce in numbers or lose functionality. It is thus important to know the intrinsic fatigue mechanism of the acellular valve leaflets in the absence of cell maintenance. Moreover, unlike the glutaraldehyde-fixed porcine valve leaflets (one type of the current bioprosthetic valves), the decellularized valve leaflets lack stabilizing exogenous crosslinks and will likely exhibit a fatigue mechanism different from those chemically treated bioprosthetic leaflets. In this study, the decellularized AVs were subjected to cardiac exercising and the exercised AV leaflets were characterized structurally and mechanically to assess the intrinsic fatigue mechanism of AV ECM in the absence of cellular maintenance.

MATERIALS AND METHODS

Sample Preparation and Decellularization Protocol

Porcine hearts were obtained from a local slaughter house and placed in phosphate buffered saline (PBS) at 4 °C for transport. The AV conduit was resected and all unneeded tissues were carefully trimmed off. The remaining valve conduit included three valve leaflets (cusps), valve annulus, Valsalva sinuses, and a portion of the ascending aorta, along with stubs of coronary arteries preserved around the coronary ostia (the two coronary arterial orifices were later sealed with sutures and cyanoacrylate glue before mounting into flow loop exerciser).

Valve conduits were subjected to decellularization with a detergent treatment protocol (sodium dodecyl sulfate, SDS), which we found to preserve the valve leaflet integrity relatively well (maintaining critical mechanical and microstructural properties).¹⁷ The valve conduits were incubated in a hypotonic Tris buffer (10 mM Tris, PH 8.0, Sigma-aldrich) with 0.1% EDTA and 1% antibiotic-antimycotic (#152400, Invitrogen) for 1 h, and then decellularized with 0.1% SDS, 1 mM phenylmethylsulfonyl fluoride (PMSF,

protease inhibitor), and RNase A (20 $\mu\text{g/ml}$) and DNase (0.2 mg/ml) in the same hypotonic Tris buffer. The decellularization lasted 48 h at room temperature with constant shaking. The decellularized tissues were then rinsed thoroughly with PBS.^{4,15}

Pulsatile Flow Loop Exerciser

A visually clear, cylindrical sample chamber was designed to allow for heart pulsatile flow condition while maintaining sterility (Fig. 1). The sample chamber was designed with a removable acrylic window to allow placement of varying diameter decellularized valve conduits prior to device assembly. Sample chamber was then attached with flow loop forming a closed fluid circuit. Pulsatile flow (50 strokes/minute) commenced with a metering bellows pump that has an adjustable stroke volume (5.5–55 mL); the diastolic pressure was 40 mmHg, and the cycle for valve opening and closing was 1.2 s. The valve conduit was sutured into a silicone root with the Valsalva sinus design (Fig. 1a), which allowed easy mounting of the decellularized valve conduit and was necessary to keep the right geometry of the valve conduit. Note that all silicone roots were custom made using the same mould and materials, thus having similar compliance. In total, three flow loops were built for the experiments. 1 liter PBS solution was added with 3% antibiotic–antimycotic and 0.1 M protease inhibitor PMSF and changed every two days to maintain sterility. The decellularized heart valves were then exposed to pulsatile pressures and flows for as long as 28 days in a sterile setting at room temperature.

Experimental Design

Two valve conduits (6 leaflets) were subjected to 2 weeks of cardiac exercising (~1.0 million cardiac

cycles) and the other 2 valve conduits were subjected to 4 weeks of exercising (~2.0 million cardiac cycles). As a control, the same numbers of valve conduits were placed in the flow loop reservoir, in which the valves were exposed to same solution environment (Table 1). For each group, a total of 6 valve leaflets were harvested and used for mechanical testings and structural characterizations. Among the 6 valve leaflets, 4 square specimens were cut from 4 valve leaflets (2 leaflets per valve) and subjected to biaxial mechanical testing; after biaxial testing, the leaflets were then used for histological study. For the left two leaflets, one leaflet was used for flexural testing; since only a tissue strip was needed for the bending device, two specimens were subjected to the flexural testing by dissecting the leaflet into 2 tissue strips along the circumferential direction. The last one leaflet was subjected to SALS fiber architecture mapping. For a thorough comparison, 2 valve conduits were tested right after the decellularization and used as a baseline; native AV leaflets from two valve conduits were also obtained and subjected to histology and fiber architecture mapping.

Thickness Measurement, Histology, and Fiber Architecture Mapping

For assessing overall dimensional changes, thickness of the valve leaflets from the exercised groups

TABLE 1. Experimental design for evaluating the fatigue mechanism of the decellularized aortic valve leaflets.

| Duration | Static control | Exercised |
|----------|----------------------------------|---------------------|
| 0 | 2 valves/6 leaflets ^a | N/A |
| 2 weeks | 2 valves/6 leaflets | 2 valves/6 leaflets |
| 4 weeks | 2 valves/6 leaflets | 2 valves/6 leaflets |

^aBaseline.

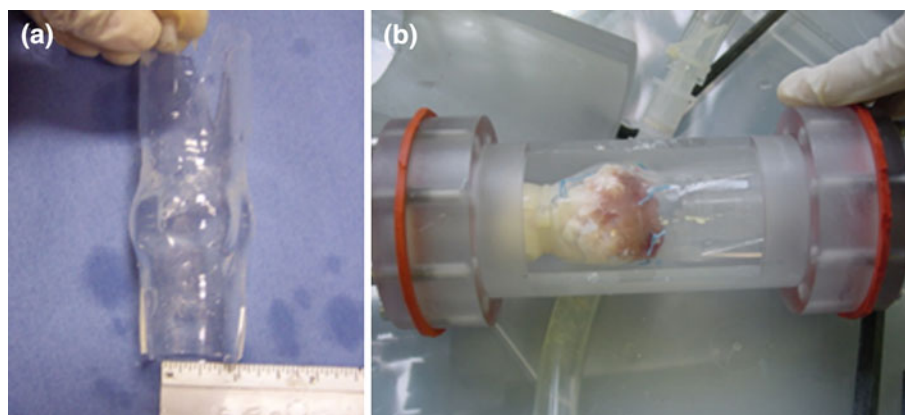


FIGURE 1. (a) A silicone root with sinus design that allows an easy mounting and proper flow conditions. (b) A cylindrical chamber for the flow loop cardiac exerciser.

(2 weeks and 4 weeks) and the static control groups (2 weeks and 4 weeks) was quantified ($N = 4$). Thickness measurements were performed using a dial caliper with an accuracy of ± 0.0254 mm. Three thickness measurements were taken in the belly region, and two thickness measurements were taken in the commissure regions. For comparison, thicknesses of the native AVs and the SDS treated AVs were also measured using the same protocol.

For histology, leaflet tissues were fixed in 4% formalin, dehydrated with graduated concentrations of ethanol, and embedded in paraffin. Transverse sections of the leaflets were subjected to hematoxylin and eosin (H&E) staining, picrosirius red staining, and Verhoeff-Van Gieson (VVG) staining. Decellularization and the fiber network were assessed with H&E stain using bright field microscopy, and picrosirius red stain using polarized light microscopy, respectively. The elastin fiber structure was assessed with VVG stain.

Small angle light scattering (SALS) technique was applied to evaluate the gross fiber architecture in valve leaflets. A detailed description of SALS and sample preparation procedure can be found in the previous publication.²⁴ Briefly, a 4 mW HeNe continuous unpolarized laser ($\lambda = 632.8$ nm) was passed through the tissue specimen. The spatial intensity distribution of the resulting scattered light represented the sum of all structural information within the light beam envelope. The angular distribution of the scattered light pattern was plotted as $I(\Phi)$, which represents distribution of fiber angles within light beam envelope. Quantifiable information based on $I(\Phi)$ includes preferred fiber direction (Φ_c) and orientation index (OI). The orientation index (OI) was defined as the angle that contains one half of the total area under the $I(\Phi)$ distribution. Normalized orientation index (NOI) was calculated using $\text{NOI} = \frac{90^\circ - \text{OI}}{90^\circ} \times 100\%$, where NOI ranged from 0% for a complete random network to 100% for a perfectly aligned network.^{17,24} SALS measurements were conducted over the entire leaflet surface in order to quantify the gross fiber structure of the leaflets. We can thus obtain a fiber architecture map, with the local degree of fiber alignment indicated by color scale (NOI value) and local preferred fiber orientation indicated by line. In the SALS map, the larger the NOI value, the higher the fiber alignment at that local region.

Biaxial Mechanical Properties

A 10 mm \times 10 mm square was dissected from the central belly region of the valve leaflet. Each side of the square specimen was mounted onto four stainless steel hooks that were attached to two loops of 000 polyester sutures. The specimens were then mounted onto the biaxial device with the circumferential and radial

directions aligned with the x_1 and the x_2 stretch axes, respectively. All testing was performed in a PBS bath (pH 7.4) at room temperature. Four fiducial graphite markers were placed in the center of the square for strain monitoring via a CCD camera. During testing, membrane tension (force per unit initial length) was applied along each axis slowly from a pre-tension, ~ 0.5 N/m, to a peak tension of 60 N/m over a rise time of 15 s. Specimens were first preconditioned for 10 contiguous cycles, following an equibiaxial protocol of $T_{CC}:T_{RR} = 60:60$ N/m, where T_{CC} and T_{RR} are the applied tensions in the circumferential and radial directions, respectively. Note that a peak tension of 60 N/m was used because it corresponds to the tension that the leaflets would experience at the physiological diastolic pressure.³⁷ Valve leaflet extensibility was characterized by λ_{CC} and λ_{RR} , the maximum stretches along circumferential and radial directions, respectively. Note that the biaxial mechanical properties of the native AV leaflets were obtained from our previous study.¹⁷

Flexural Properties

Bidirectional flexure deformation takes place in the AVL opening and closing cycles. Flexural mechanical properties reflect tissue properties and coupling of different leaflet layers. Flexural properties of the exercised AVL and controls were assessed using a bending device.^{10,20} Rectangular strips were dissected from the central belly region, with the strips cut parallel to the circumferentially oriented collagen fibers. Three fiducial graphite particles were pasted on the side of the strip with cyanoacrylate. Hollow posts were pasted on both ends of the rectangular sample and served as two anchor points, one placed on the fixed post and one placed on a bending bar. Two graphite particles were pasted on the anchor points as the final two markers for computing the curvature. During testing, the fixed post was moved towards the bending bar by a motorized stage. As the sample flexed, the bending bar deflected, which represented the amount of force exerted on the sample. It is known that the AVL shows a natural curvature in the unloaded state. In the testing, each specimen was flexed in two directions: one test bended the leaflet strip along “with curvature (WC)” direction that subjected the ventricularis to tension, and another test bended the leaflet strip along “against curvature (AC)” direction that subjected the fibrosa to tension.

Statistics

The experimental data were presented as mean \pm STDEV. Statistical analyses were performed with One

Way Analysis of Variances (ANOVA) (SigmaStat 3.0, SPSS Inc., Chicago, IL). The Holm-Sidak Test, which can be used for pair wise comparisons and comparisons versus a control group, was used for the post hoc comparison. Results were considered significantly different at $p < 0.05$. Due to the limited number of leaflets, it was necessary that we allocated the usage of the leaflets in different assessments to maximize the important information that showed structural/mechanical changes. As described above, the majority of samples were used for mechanical characterizations and histology; only one leaflet was subjected to SALS, thus no statistical analysis was performed for SALS study.

RESULTS

After cardiac exercising, the general morphology and overall fiber bundle architecture were still maintained and leaflets were able to coapt and support load; however, exercised AV leaflets exhibited unfolded and thinned morphology (Fig. 2 and Table 2). Note that

unfolding and thinning were not obvious in the static controls, which were exposed to same aqueous environment for 2 weeks or 4 weeks (Fig. 2). Ultrastructural changes of the exercised valve leaflets had been revealed by histology. After cardiac exercising, the collagen fiber network was found to be stretched out and exhibiting a more straightened morphology (Fig. 3). The disappearance of collagen crimp period was verified by the picrosirius stained slides under polarized light (Fig. 3). In contrast, collagen network in the static controls did not show the same fiber straightening morphology, but exhibited a disarrayed collagen network (Fig. 3).

VVG staining showed the loss of elastin fibers in the 4-weeks flow loop exercised leaflets (Fig. 4c). However, elastin fibers (black color) were still partially preserved in the static controls exposed to the same solution environment (Fig. 4b), which implied that elastin fiber loss in the exercised leaflets was likely related to mechanical fatigue. The VVG stained section also showed a stretched morphology of collagen (pink color) in the flow loop exercised leaflets (Fig. 4c) when compared with native and static controls (Figs. 4a, 4b);

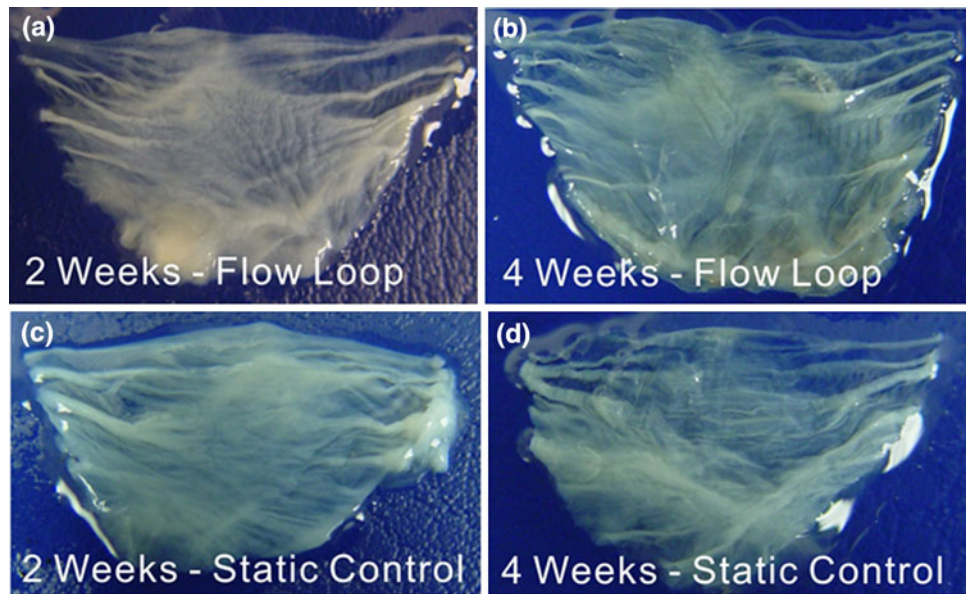


FIGURE 2. Morphology of the exercised valve leaflet showed unfolding and thinning: (a) 2-week exercising, (b) 4-week exercising. Morphology of the static control that was subjected to the same solution condition: (c) 2-week control, (d) 4-week control.

TABLE 2. Comparison of the valve leaflet thickness.

| | | Thickness of Valve Leaflets (mm) | | | |
|-------------|----------------------------|----------------------------------|-----------------------------|-----------------------------|-----------------------------|
| Native | SDS treatment | Ctrl-2 weeks | Ctrl-4 weeks | FL-2 weeks | FL-4 weeks |
| 0.46 ± 0.12 | 0.44 ± 0.09 $p = 0.709$ | 0.29 ± 0.03* $p = 0.004$ | 0.31 ± 0.03* $p = 0.011$ | 0.22 ± 0.04* $p < 0.001$ | 0.24 ± 0.08* $p < 0.001$ |

* Denotes statistical significance when compared with the thickness of the native valve leaflet (third row gives p values). Thinning and stretched morphology of the flow loop exercised leaflets was verified by the decreased leaflet thickness.

moreover, layered delamination was evidenced in the exercised leaflets (Fig. 4c). Other than the intuitive histological observations, SALS fiber architecture map verified a straightening of the fiber network. Flow loop exercised leaflets were found to have a higher overall fiber alignment due to cyclic stretching (Fig. 5c, 5e), while the static controls showed a trend of decreased fiber alignment along with the storage time (Fig. 5d, 5f).

Tissue extensibility along the circumferential and radial direction of the valve leaflet was determined from the maximum stretch at 60 N/m equibiaxial tension. Biaxial testing showed that (i) the extensibility along both circumferential and radial directions increased after SDS treatment, however, (ii) the extensibility was reduced by solution storage effects (static control groups), and (iii) the extensibility was further reduced by cardiac exercising (2 weeks and 4 weeks cardiac cycling) (Fig. 6). A further reduction in the extensibility in the static control group did not occur past 2 weeks

(Fig. 6). There were no obvious changes in the flexural properties after 2 and 4 weeks flow loop exercising, and the valve leaflets still demonstrated a nonlinear response when flexed in both WC and AC directions (Fig. 7). Note that a stiffer linear response was observed in native aortic valve leaflets.¹⁷

DISCUSSION

It is a challenge to characterize the material fatigue of biological tissues that undergo cyclic mechanical loading. In the *in vivo* animal or human subject experiments, many biofactors were found to interact with the tissue implants and result in compositional and structural changes that will affect the outcome. For example, inflammatory response, fibrosis, and calcification alter the structure and composition of TEHVs and hence the outcome of valve implants.^{32,34,38,39} *In vitro* fatigue

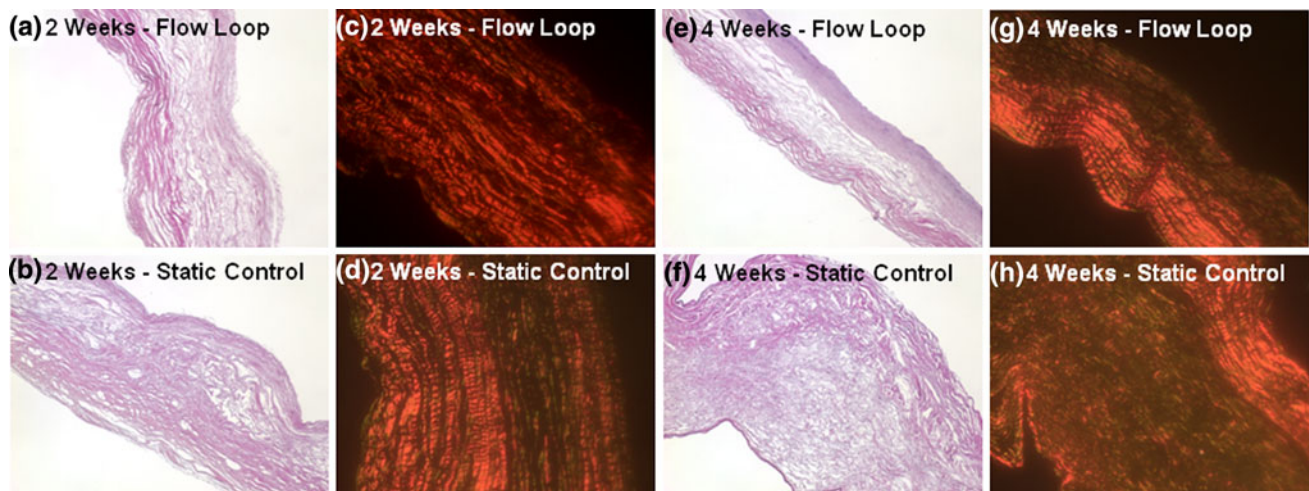


FIGURE 3. Histology showed the straightening of collagen fibers in the exercised leaflets. H&E images for (a) 2-week exercising and (b) 2-week static control; polarized light images (picrosirius red-stained section) for (c) 2-week exercising and (d) 2-week static control. H&E images for (e) 4-week exercising and (f) 4-week static control; polarized light images (picrosirius red-stained section) for (g) 4-week exercising and (h) 4-week static control.



FIGURE 4. Verhoeff-Van Gieson staining revealed the elastin loss in the flow loop exercised leaflets. (a) Native valve leaflet, (b) 4-week static control, and (c) 4-week exercising. Black: elastin, Red: Collagen, F: Fibrosa, V: Ventricularis.

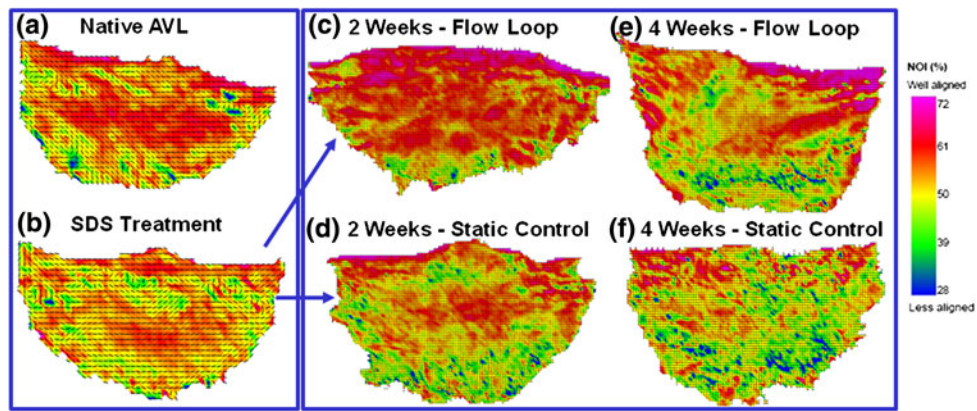


FIGURE 5. Fiber architecture mapped by small angle light scattering showed that the exercised leaflet had a higher fiber alignment (larger NOI corresponds to higher alignment). (a) Native valve leaflet, (b) leaflet right after SDS decellularization treatment, (c) leaflet after 2-week exercising, (d) 2-week static control, (e) leaflet after 4-week exercising, and (f) 4-week static control.

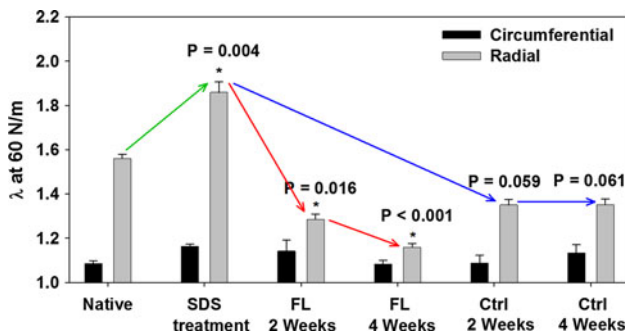


FIGURE 6. Comparison of the valve leaflet extensibility among the native, SDS-treated, 2-week flow loop exercised, 4-week flow loop exercised, 2-week static control, and 4-week static control groups. Biaxial testing showed that (i) the leaflet extensibility along both circumferential and radial directions increased after SDS treatment; however, (ii) the leaflet extensibility was reduced by solution storage effects (static control groups), and (iii) the leaflet extensibility was further reduced by cardiac exercising (2 weeks and 4 weeks cardiac cycling).

experiments have not been carried out often possibly due to the concern on biological tissue degeneration during the period of mechanical cycling.

In order to assess the intrinsic fatigue mechanism of AV ECM, we designed an in vitro approach that differentiated the mechanical effect from other factors. There were three key components in our experimental design: (i) A flow loop was used to apply the cyclic opening and closing to the acellular valve leaflets in a pulsatile flow condition; (ii) the circulating solution with 3% antibiotic-antimycotic and 0.1 M protease inhibitor PMSF was changed every 2 days to maintain a sterile environment; and (iii) a valve conduit was sat in the flow loop reservoir as a static control to exclude the effects of solution storage.

Without cellular maintenance, irreversible structural disruption occurred in the acellular valve leaflets after 2-week and 4-week cyclic exercising. Undulation in the AV fibrosa layer was found to be unfolded and valve

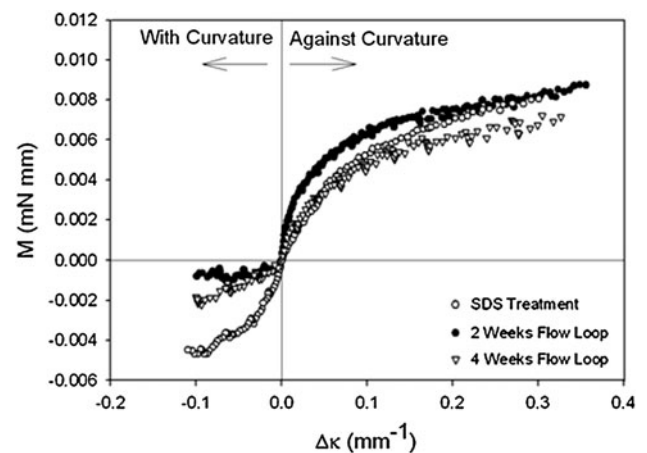


FIGURE 7. No obvious changes in flexural properties after 2 and 4 weeks flow loop exercising. The exercised valve leaflets still demonstrated a nonlinear response when flexed in both WC and AC directions. Note that a stiffer linear response was observed in the native aortic valve leaflets.¹⁷

leaflet showed a thinned morphology overall. The histological observation revealed that the collagen fiber network was stretched out and the collagen crimp period diminished due to fiber straightening. These underlying structural alterations explained the thinned and stretched morphology in the exercised leaflets. Our thickness measurement quantitatively supported the observation on leaflet thinning after cyclic exercising (Table 2). Furthermore, considering the conservation of leaflet mass, stretching of the leaflet could also be deduced from the fact that the leaflets were thinned and the crimped fibers were straightened. Note that the static control groups also showed a degree of thickness reduction (Table 2); one speculation about the effects of solution storage is the further depletion of proteoglycans during the storage, which could be a reason that static controls showed a slight thickness decrease. Nevertheless, the amount of thickness reduction in the

exercised leaflets was significantly greater than the static controls (Table 2), indicating the effect of cyclic exercising.

The initial collagen crimp configuration in the unloaded leaflet and the later uncrimping mechanism provide a flexible leaflet deformation without incurring large internal tissue stress.^{14,18,19} This behavior is consistent with the uncrimping mechanism in tendon/ligament tissues, which generates a nonlinear J-shape (concave-upward) stress–strain curve.⁹ The loss of collagen crimp structure in the leaflets results in a less extensible and stiffer tissue behavior, consequently altering the opening and closing performance of AVs.

Moreover, we found that elastin fibers were reduced in the flow loop exercised leaflets (Fig. 4c), while the elastin fibers were partially preserved in the static control that was subjected to the same solution environment (Fig. 4b). It is still unknown exactly how mechanical fatigue triggered the reduction of elastin fibers in the flow loop exercised leaflets. One possibility is that mechanical fatigue might cause elastin fiber damage/fragmentation, which in turn accelerated the disruption of both the collagen and elastin networks (Fig. 4c). Our observation echoes the study by Lee *et al.*,¹⁶ which reported that damage to the elastin would likely enable the collagen network to elongate (corresponding to the stretched morphology we observed here), reducing valve cusp extensibility. Thus, it could be concluded that, in this *in vitro* study, degradation alone could not explain the reduction of elastin in the exercised leaflets. We speculated that,

along with degradation, mechanical factors accelerated the reduction of elastin fibers in a fiber network lacking stabilizing crosslinks; the loss of elastin in turn aggravated the leaflet unfolding and the straightening of collagen fibers. Delaminating of AV layers was also observed in the histology of the exercised leaflets (Fig. 4c). SALS results further confirmed the straightening of the fiber network; the 2-week exercised sample showed very high NOIs across the leaflet (Fig. 5c); for the 4-week exercised leaflet, regions close to the annulus showed lower NOIs (Fig. 5e), which could be due to the regional structural damage over the limit of fiber straightening, e.g., delamination (Fig. 4c). The reduction of overall NOIs in the static controls (Fig. 5d, 5f) was likely due to the effects of solution storage that need further investigation.

A schematic illustration of the collagen fiber network disruption after decellularization and the fiber straightening after cardiac exercising was shown in Fig. 8. Our previous study showed that, after SDS decellularization treatment, the collagen fibers were still locally crimped, but no longer showed the macroscopically organized light-distinguishing bands.¹⁷ Note that, however, no dimension change was found in the valve leaflets right after SDS treatment.¹⁷ After SDS decellularization, the partially disrupted collagen fiber network and the same reference status were believed to be the underlying mechanism of a larger tissue extensibility (Fig. 8b).¹⁷ Note that the reference status referred to the original dimension of the leaflet that was used to calculate the stretch. In the exercised leaflets, however,

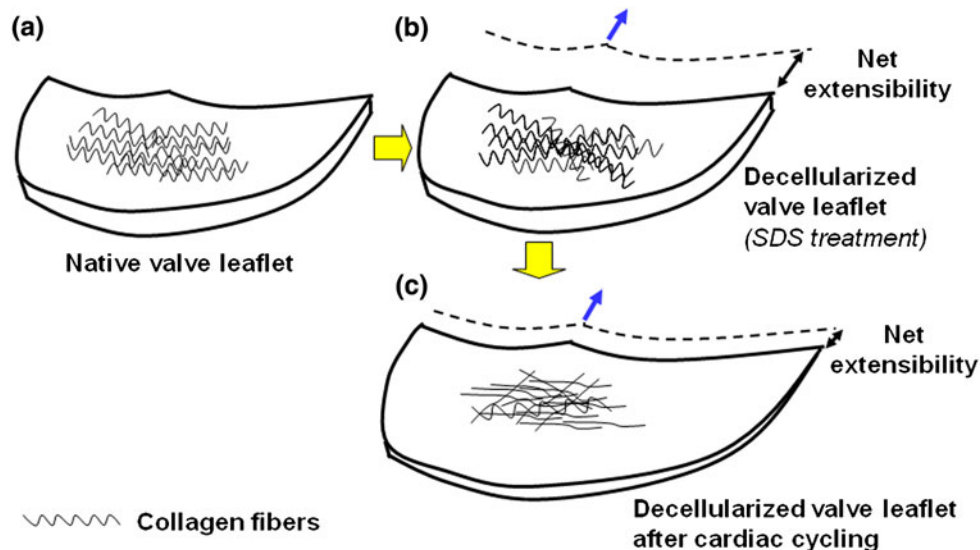


FIGURE 8. A schematic illustration of the underlying structural mechanism for net extensibility changes. (a) Native aortic valve leaflet, (b) Decellularized leaflet right after SDS treatment, and (c) Decellularized valve leaflet after cardiac cycling. Note that the sketches of collagen fibers were simplified for illustration purpose. Refer to the histology in this study and our previous study¹⁷ for the details of collagen fiber organization.

unfolding and straightening of collagen undulations produced a thinned and stretched morphology. Mechanically, the structural alteration changed the reference status of the exercised leaflet and consequently caused a lower net tissue extensibility (Fig. 8c). The lower net tissue extensibility was observed in the exercised valve leaflets in the biaxial mechanical characterization. The extensibility of the acellular valve leaflets decreased after 2-week cardiac exercising, and further reduced after 4-week cardiac cycling (Fig. 6).

Our study showed that, in the absence of cellular maintenance, decellularized valve leaflets experience irreversible structural deterioration due to lack of exogenous stabilizing crosslinks. This finding implied that recellularization is a key for the successful development of TEHV using a tissue-derived scaffold via decellularization approach. Without the maintenance of functioning aortic valve interstitial cells (AVICs), the scaffold damages accumulated in the cyclic fatigue cannot be repaired timely, and overall structural disruption takes place along with time. As we know, each heart valve opens and closes at least 3×10^9 times during an average lifetime, which demonstrates the valve's remarkable intrinsic ability to withstand mechanical loading by continual remodeling and repair of the valvular ECM. This homeostatic maintenance of the valve ECM is accomplished by the AVICs. AVICs are plastic and reversible as the cells are synthetically active (MMP13+/SMA+) during the states of valvular tissue development, adaptation, and disease, while in normal valves, the cells were found to be quiescent.²¹ If the local stress concentration is higher than the physiological range, the abnormal mechanical stimuli might activate the AVICs to deposit more ECM. From biomechanical perspective, the newly deposited ECM will likely reduce the local stress and hence maintain an optimal stress distribution. The lack of repairing and remodeling capabilities allows a vicious cycle and occurrence of permanent structural alteration (e.g., fiber straightening and loss of local crimp structure).

In the experiments, contamination was found in one flow loop experiment and abnormal opening and closing was found in another flow loop experiment. The contaminated leaflets and torn leaflets were excluded from analysis and two experiments were repeated to obtain the planned samples size (see Table 1). The cardiac exercising experiment was performed at room temperature, which likely caused more aggressive solution storage effects in the valve conduits than that in an environment of 4 °C. Future improvements of the experimental setup might be to apply environmental temperature control for the cardiac exerciser. If a long-term flow loop exercising is needed, the environmental temperature can be set at

4 °C; or, if the physiological condition is more of a concern, the environmental temperature can be set at 37 °C and the blood rheology can be taken into consideration by using flow loop solution that mimics the rheological properties of blood.

One limitation of this study was the low sample number in SALS characterization, i.e., only one leaflet was used for SALS fiber architecture mapping. However, the structural alterations revealed by SALS were consistent with the histological observation, and we thus reported it as complementary data further confirming fiber unfolding and straightening. Nevertheless, future study with higher sample number is warranted to further confirm our SALS observation. Although thorough structural and mechanical evaluations have been carried out in our study, biochemical characterizations such as glycosaminoglycan and collagen assessments might further help us understanding the leaflet tissue disruption/degeneration.

It is worthy to point out that the in vitro cardiac exerciser still represents a harsh environment in which effects of solution storage cannot be fully excluded (also note that this in vitro cardiac exerciser is not designed for physiological modeling purpose). Consequently, the in vitro ECM fatigue takes place in an accelerated fashion. *It is thus not appropriate to extrapolate the AV ECM fatigue rate observed in this in vitro study to the durability of valve implants.* Indeed, the fate of acellular valve implants⁸ or TEHV^{26,42} in animals or in human subjects is a more complicated issue that warrants future investigations.

CONCLUSIONS

In this study, we found that, without cellular maintenance, the exercised AV leaflets showed an unfolded and thinned morphology. Ultrastructural observation and SALS fiber architecture mapping verified the straightening of the fiber network after cyclic fatigue. Loss of elastin fibers in the exercised leaflet was also observed, which likely accelerate the unfolding of collagen undulation and straightening of fibers. The structural alteration caused a changed leaflet reference status and resulted in lower net tissue extensibility in the exercised leaflets. We conclude that, in the absence of cellular maintenance, decellularized valve leaflets experience a structural deterioration due to the lack of exogenous stabilizing crosslinks and the structural disruption is irreversible and cumulative. Our finding implies the importance of recellularization in developing a TEHV, in which long term durability will likely be better achieved by continual remodeling and repair of the valvular ECM.

ACKNOWLEDGMENT

This work is supported by American Heart Association (BGIA-0565346U) and Health Resources and Services Administration (DHHS R1CRH10429-01-00). JL is supported in part by NIH NL097321. The authors would like to thank Dr. Steve Elder for help and invaluable discussion.

CONFLICT OF INTEREST

All authors declare that there are no proprietary, financial, professional or other personal conflicts of interest that could inappropriately influence (bias) the work presented in this manuscript.

REFERENCES

- ¹Angell, W. W., J. H. Oury, C. G. Duran, and C. Infantes-Alcon. Twenty-year comparison of the human allograft and porcine xenograft. *Ann. Thorac. Surg.* 48(3 Suppl): S89–S90, 1989.
- ²Bader, A., T. Schilling, O. E. Teebken, G. Brandes, T. Herden, G. Steinhoff, *et al.* Tissue engineering of heart valves—human endothelial cell seeding of detergent acellularized porcine valves. *Eur. J. Cardiothorac. Surg.* 14(3): 279–284, 1998.
- ³Bertipaglia, B., F. Ortolani, L. Petrelli, G. Gerosa, M. Spina, P. Pauletto, *et al.* Cell characterization of porcine aortic valve and decellularized leaflets repopulated with aortic valve interstitial cells: the VESALIO Project (Vitalitate Exornatum Succedaneum Aorticum Labore Ingenioso Obtenibitur). *Ann. Thorac. Surg.* 75(4):1274–1282, 2003.
- ⁴Booth, C., S. A. Korossis, H. E. Wilcox, K. G. Watterson, J. N. Kearney, J. Fisher, *et al.* Tissue engineering of cardiac valve prostheses I: development and histological characterization of an acellular porcine scaffold. *J. Heart Valve Dis.* 11(4):457–462, 2002.
- ⁵Cannegieter, S., F. Rosendaal, and E. Briet. Thromboembolic and bleeding complications in patients with mechanical heart valve prostheses. *Circulation* 89:635–641, 1994.
- ⁶Cebotari, S., H. Mertsching, K. Kallenbach, S. Kostin, O. Repin, A. Batrinac, *et al.* Construction of autologous human heart valves based on an acellular allograft matrix. *Circulation* 106(12 Suppl 1):I63–I68, 2002.
- ⁷Courtman, D. W., C. A. Pereira, S. Omar, S. E. Langdon, J. M. Lee, and G. J. Wilson. Biomechanical and ultrastructural comparison of cryopreservation and a novel cellular extraction of porcine aortic valve leaflets. *J. Biomed. Mater. Res.* 29(12):1507–1516, 1995.
- ⁸da Costa, F. D., A. C. Costa, R. Prestes, A. C. Domanski, E. M. Balbi, A. D. Ferreira, *et al.* The early and midterm function of decellularized aortic valve allografts. *Ann. Thorac. Surg.* 90(6):1854–1860, 2010. doi:S0003-4975(10)01872-2[pil]10.1016/j.athoracsur.2010.08.022.
- ⁹Fung, Y. C. *Biomechanics: Mechanical Properties of Living Tissues*. New York: Springer, 1981.
- ¹⁰Gloeckner, D. C., K. L. Billiar, and M. S. Sacks. Effects of mechanical fatigue on the bending properties of the porcine bioprosthetic heart valve. *ASAIO J.* 45(1):59–63, 1999.
- ¹¹Grabow, N., K. Schmohl, A. Khosravi, M. Philipp, M. Scharfschwerdt, B. Graf, *et al.* Mechanical and structural properties of a novel hybrid heart valve scaffold for tissue engineering. *Artif. Organs.* 28(11):971–979, 2004.
- ¹²Hammermeister, K., G. K. Sethi, W. G. Henderson, F. L. Grover, C. Oprian, and S. H. Rahimtoola. Outcomes 15 years after valve replacement with a mechanical versus a bioprosthetic valve: final report of the Veterans Affairs randomized trial. *J. Am. Coll. Cardiol.* 36(4):1152–1158, 2000.
- ¹³Hoerstrup, S. P., R. Sodian, S. Daebritz, J. Wang, E. A. Bacha, D. P. Martin, *et al.* Functional living trileaflet heart valves grown in vitro. *Circulation* 102(19 Suppl 3):III44–III49, 2000.
- ¹⁴Joyce, E. M., J. Liao, F. J. Schoen, J. E. Mayer, Jr., and M. S. Sacks. Functional collagen fiber architecture of the pulmonary heart valve cusp. *Ann. Thorac. Surg.* 87(4): 1240–1249, 2009. doi:S0003-4975(08)02694-5[pil]10.1016/j.athoracsur.2008.12.049.
- ¹⁵Korossis, S. A., C. Booth, H. E. Wilcox, K. G. Watterson, J. N. Kearney, J. Fisher, *et al.* Tissue engineering of cardiac valve prostheses II: biomechanical characterization of decellularized porcine aortic heart valves. *J. Heart Valve Dis.* 11(4):463–471, 2002.
- ¹⁶Lee, T. C., R. J. Midura, V. C. Hascall, and I. Vesely. The effect of elastin damage on the mechanics of the aortic valve. *J. Biomech.* 34(2):203–210, 2001. doi:S0021-9290(00)00187-1[pil].
- ¹⁷Liao, J., E. M. Joyce, and M. S. Sacks. Effects of decellularization on mechanical and structural properties of the porcine aortic valve leaflets. *Biomaterials* 29(8):1065–1074, 2008.
- ¹⁸Liao, J., L. Yang, J. Grashow, and M. S. Sacks. Molecular orientation of collagen in intact planar connective tissues under biaxial stretch. *Acta Biomater.* 1(1):45–54, 2005.
- ¹⁹Liao, J., L. Yang, J. Grashow, and M. S. Sacks. The relation between collagen fibril kinematics and mechanical properties in the mitral valve anterior leaflet. *J. Biomech. Eng.* 129(1):78–87, 2007.
- ²⁰Lovekamp, J. J., D. T. Simionescu, J. J. Mercuri, B. Zubiate, M. S. Sacks, and N. R. Vyavahare. Stability and function of glycosaminoglycans in porcine bioprosthetic heart valves. *Biomaterials* 27(8):1507–1518, 2006.
- ²¹Rabkin-Aikawa, E., M. Aikawa, M. Farber, J. R. Kratz, G. Garcia-Cardena, N. T. Kouchoukos, *et al.* Clinical pulmonary autograft valves: pathologic evidence of adaptive remodeling in the aortic site. *J. Thorac. Cardiovasc. Surg.* 128(4):552–561, 2004.
- ²²Rajani, B., R. B. Mee, and N. B. Ratliff. Evidence for rejection of homograft cardiac valves in infants. *J. Thorac. Cardiovasc. Surg.* 115(1):111–117, 1998.
- ²³Sacks, M. S., F. J. Schoen, and J. E. Mayer. Bioengineering challenges for heart valve tissue engineering. *Annu. Rev. Biomed. Eng.* 11:289–313, 2009. doi:10.1146/annurev-bioeng-061008-124903.
- ²⁴Sacks, M. S., D. B. Smith, and E. D. Hiester. A small angle light scattering device for planar connective tissue microstructural analysis. *Ann. Biomed. Eng.* 25(4):678–689, 1997.
- ²⁵Schoen, F. J. Pathology of heart valve substitution with mechanical and tissue prostheses. In: *Cardiovascular Pathology*, edited by M. D. Silver, A. I. Gotlieb, and F. J. Schoen. New York: Livingstone, 2001.
- ²⁶Schoen, F. J. Heart valve tissue engineering: quo vadis? *Curr. Opin. Biotechnol.* 2011. doi:S0958-1669(11)00018-8[pil]10.1016/j.copbio.2011.01.004.

- ²⁷Schoen, F., and R. Levy. Tissue heart valves: current challenges and future research perspectives. *J. Biomed. Mater. Res.* 47:439–465, 1999.
- ²⁸Schoen, F., R. Levy, and H. Piehler. Pathological considerations in replacement cardiac valves. *Cardiovasc. Pathol.* 1(1):29–52, 1992.
- ²⁹Senthilnathan, V., T. Treasure, G. Grunkemeier, and A. Starr. Heart valves: which is the best choice? *Cardiovasc. Surg.* 7(4):393–397, 1999.
- ³⁰Shinoka, T., C. K. Breuer, R. E. Tanel, G. Zund, T. Miura, P. X. Ma, *et al.* Tissue engineering heart valves: valve leaflet replacement study in a lamb model. *Ann. Thorac. Surg.* 60(6 Suppl):S513–S516, 1995.
- ³¹Sodian, R., S. P. Hoerstrup, J. S. Sperling, S. Daebritz, D. P. Martin, A. M. Moran, 19 Suppl 3, *et al.* Early In vivo experience with tissue-engineered trileaflet heart valves. *Circulation* 102(19 Suppl 3):III22–III29, 2000.
- ³²Spina, M., F. Ortolani, A. E. Messlemani, A. Gandaglia, J. Bujan, N. Garcia-Honduvilla, *et al.* Isolation of intact aortic valve scaffolds for heart-valve bioprostheses: extracellular matrix structure, prevention from calcification, and cell repopulation features. *J. Biomed. Mater. Res. A.* 67(4):1338–1350, 2003.
- ³³Stamm, C., A. Khosravi, N. Grabow, K. Schmohl, N. Treckmann, A. Drechsel, *et al.* Biomatrix/polymer composite material for heart valve tissue engineering. *Ann. Thorac. Surg.* 78(6):2084–2093, 2004.
- ³⁴Steinhoff, G., U. Stock, N. Karim, H. Mertsching, A. Timke, R. R. Meliss, *et al.* Tissue engineering of pulmonary heart valves on allogenic acellular matrix conduits: in vivo restoration of valve tissue. *Circulation* 102(19 Suppl 3):III50–III55, 2000.
- ³⁵Stock, U. A., M. Nagashima, P. N. Khalil, G. D. Nollert, T. Herden, J. S. Sperling, *et al.* Tissue-engineered valved conduits in the pulmonary circulation. *J. Thorac. Cardiovasc. Surg.* 119(4 Pt 1):732–740, 2000.
- ³⁶Stock, U. A., J. P. Vacanti, J. E. Mayer, Jr., and T. Wahlers. Tissue engineering of heart valves—current aspects. *Thorac. Cardiovasc. Surg.* 50(3):184–193, 2002.
- ³⁷Thubrikar, M. *The Aortic Valve*. Boca Raton: CRC, 1990.
- ³⁸Vesely, I. Heart valve tissue engineering. *Circ. Res.* 97:743–755, 2005.
- ³⁹Wilson, G. J., D. W. Courtman, P. Klement, J. M. Lee, and H. Yeger. Acellular matrix: a biomaterials approach for coronary artery bypass and heart valve replacement. *Ann. Thorac. Surg.* 60(2 Suppl):S353–S358, 1995.
- ⁴⁰Wilson, G. J., H. Yeger, P. Klement, J. M. Lee, and D. W. Courtman. Acellular matrix allograft small caliber vascular prostheses. *ASAIO Trans.* 36(3):M340–M343, 1990.
- ⁴¹Yacoub, M., N. R. Rasmi, T. M. Sundt, O. Lund, E. Boyland, R. Radley-Smith, *et al.* Fourteen-year experience with homovital homografts for aortic valve replacement. *J. Thorac. Cardiovasc. Surg.* 110(1):186–193, 1995; (discussion 93-4).
- ⁴²Yacoub, M. H., and J. J. Takkenberg. Will heart valve tissue engineering change the world? *Nat. Clin. Pract. Cardiovasc. Med.* 2(2):60–61, 2005. doi:[ncpcardio0112](https://doi.org/10.1038/ncpcardio0112)[pii] [10.1038/ncpcardio0112](https://doi.org/10.1038/ncpcardio0112).
- ⁴³Yannas, I. *Natural Materials*. Biomaterial Science. San Diego: Academic Press, 1996.
- ⁴⁴Zeltinger, J., L. K. Landeen, H. G. Alexander, I. D. Kidd, and B. Sibanda. Development and characterization of tissue-engineered aortic valves. *Tissue Eng.* 7(1):9–22, 2001.